REVIEW

A precise, three-dimensional atlas of myocardial perfusion correlated with coronary arteriographic anatomy

Yuko Nakagawa, MD,[a] Keiichi Nakagawa, MD,[b] Stefano Sdringola, MD,[c,d] Nizar Mullani, BS,[c] and K. Lance Gould, MD[c,d]

To map precise myocardial perfusion anatomy, we correlated detailed coronary arteriographic anatomy for every coronary artery and all secondary branches in the heart that had flow-limiting stenosis with corresponding specific, circumscribed, myocardial perfusion defects by positron emission tomography. Eight hundred ninety-five patients with abnormal coronary arteriograms showing any visible coronary artery narrowing of greater than 10% diameter stenosis underwent positron emission tomography perfusion imaging at rest and after dipyridamole stress; the data obtained were processed automatically into 3-dimensional topographic displays of relative radionuclide uptake in anterior, septal, left lateral, and inferior quadrant views, without attenuation artifacts, depth-dependent resolution, or spatial distortion of polar displays. The selection criterion for detailed anatomic analysis was the presence of a discrete, localized, moderate to severe, dipyridamole-induced perfusion defect, defined by automated algorithms as 1 quadrant view outside 2 SDs of healthy control subjects with which a specific stenotic coronary artery and/or its secondary branches could be correlated unequivocally on the coronary arteriogram for mapping precise perfusion anatomy, not for determining sensitivity or specificity.

Because the anatomy of myocardial perfusion is inherently not statistical data, the results are presented as a summary atlas and series of individual cases that illustrate myocardial perfusion anatomy. Because the patterns of myocardial perfusion anatomy were derived from a large number of subjects, the atlas provides generalized information, not previously published, that correlates detailed arteriographic anatomy with perfusion anatomy including secondary diagonal, marginal, and posterior descending branches of the coronary arteries. (J Nucl Cardiol 2001;8:580-90.)

Key Words: Myocardial perfusion • coronary artery disease • positron emission tomography • myocardial perfusion anatomy • coronary arteriography • coronary arterial anatomy

Reviewing detailed myocardial perfusion anatomy is appropriate for several reasons. First, the limitations of coronary arteriography for identifying and defining severity of coronary atherosclerosis are well documented[1,2] and include the following: (1) errors in visually estimated percent diameter narrowing,[1,2] (2) extensive disease in the supposed normal reference segment (as determined by intravascular ultrasonography), such that relative percent narrowing is of little value,[3-5] (3) errors of 50% to 80% with the use of coronary arteriography in identifying diffuse coronary artery disease,[3-5] and (4) failure of arteriography to account for the hemodynamic effects of multiple stenoses or mixed segmental and diffuse disease.[2]

Second, sufficient clinical experience has been gained with the use of positron emission tomography (PET) to map precise myocardial perfusion anatomy without attenuation artifacts, which is also valuable for interpreting single photon emission tomography results.

From the Third Department of Internal Medicine, Chiba University School of Medicine, Chiba,[a] and Nishidai Clinic Diagnostic Imaging Center, Tokyo,[b] Japan; The Memorial Hermann Health Care System and Hermann Hospital and Department of Medicine[c] and Weatherhead PET Center for Preventing and Reversing Atherosclerosis,[d] University of Texas Medical School, Houston, Tex.

Supported in part by NIH grant R01 HL48574, The Weatherhead Endowment, and The Memorial Hermann Foundation.

Reprint requests: K. Lance Gould, MD, The Weatherhead PET Center, The University of Texas Medical School, Room 4.256 MSB, Houston, TX 77030; *gould@pet.med.uth.tmc.edu.*

1071-3581/2001/$35.00 + 0 **43/1/115093**
doi:10.1067/mnc.2001.115093

Third, in randomized trials carried out during the past 10 years, vigorous cholesterol-lowering has stopped progression, caused regression, and reduced cardiovascular events or deaths in 40% to 90% of patients, thereby providing the basis for vigorous noninvasive management of coronary artery disease.[1,2] In the Randomised Intervention Treatment of Angina (RITA-2),[6] Veterans Affairs Non-Q-Wave Infarction Strategies in Hospital (VANQWISH),[7] and Atorvastatin Versus Revascularization Treatments (AVERT) trials,[8] angioplasty procedures or bypass surgery had significantly poorer adverse outcomes of death and myocardial infarction than intense medical treatment, even in cases of severe stenosis averaging 81% in diameter (AVERT). In the 8-year follow-up of the Familial Atherosclerosis Treatment Study (FATS) trial[9] and in our experience, intense lipid and risk factor treatment reduced deaths, cardiac events, and/or invasive procedures by 90% compared with those in control groups who received the usual care. Consequently, definitive noninvasive diagnosis and intense lipid and risk factor treatment make determination of precise perfusion anatomy clinically important.

Finally, recurrent angina is common after bypass surgery or angioplasty because of graft closure, restenosis, progressive disease proximal to bypass grafts, diffuse coronary atherosclerosis, other stenosis not addressed by the procedure, or endothelial dysfunction without localized flow-limiting stenoses. For such complex anatomy, pathophysiology, and/or perfusion patterns, a precise perfusion map commonly identifies the precise artery and stenosis for further focal procedures for angina that is resistant to treatment.

Therefore from a database of 895 patients we developed a precise, detailed perfusion atlas for every coronary artery and all secondary branches by correlating distinct, localized moderate to severe myocardial perfusion defects objectively quantified on 3-dimensional (3D) PET perfusion images with every specific coronary artery and its individual branches on coronary arteriograms.

METHODS

Study Subjects

After informed consent approved by the institutional review committee, 895 men and women, aged 28 to 88 years, who were being clinically evaluated for coronary artery disease underwent coronary arteriography and myocardial perfusion imaging by PET at rest and after dipyridamole with nitrogen 13 (N-13) ammonia. Selection criteria for detailed anatomic correlations included moderate to severe, definite, circumscribed perfusion defects, defined by automated objective computer algorithms as at least 1 quadrant of the 3D myocardial display outside 2 SDs of normal values. Selected perfusion defects also had to be associated with a coronary arteriogram with a specific artery or specific branches with narrowing greater than 10% diameter stenosis by visual inspection corresponding to the distribution of the myocardial perfusion defect. These criteria allowed for identification of the anatomic artery for the map of perfusion anatomy.

In view of the documented limitations of coronary arteriography for identifying and/or assessing severity of combined diffuse and multisegmental coronary artery disease,[2] the arteriograms in these patients were used to identify the specific anatomic arteries or branches with any visually apparent coronary artery narrowing of over 10% diameter stenosis, without controversies about quantitative severity or accuracy even though stenoses were typically quite severe as a result of the criterion of moderate to severe perfusion defects for selection of patients. The arteriograms were analyzed visually only for the anatomic identity and location of a coronary artery or branch corresponding to a moderate or severe myocardial perfusion defect. The purpose was not to determine sensitivity and specificity, which depend on severity criteria of both arteriographic and perfusion abnormalities, but rather to determine the anatomic correspondence of arteriographic anatomy with definite, circumscribed perfusion defects.

Positron Emission Tomography

PET imaging of myocardial perfusion at rest and after dipyridamole was carried out as previously described,[2,10-12] with the use of the University of Texas–designed bismuth germanium oxide (Posicam, Positron Corp) or cesium fluoride multislice scanner with N-13 ammonia before and after intravenous dipyridamole (0.142 mg/kg/min for 4 minutes).

Automated Quantitative Analysis of PET

Completely automated analysis of severity of PET abnormalities was carried out with previously described software.[2,10-13] A 3D restructuring algorithm generated true short-axis and long-axis views from PET transaxial cardiac images, perpendicular to and parallel to the long axis of the left ventricle. To avoid the visual spatial distortion inherent in polar displays, we used the circumferential profiles to reconstruct 3D topographic views of the left ventricle, reflecting relative regional activity distribution at rest and after dipyridamole stress.

The 3D topographic views are divided into fixed sections consisting of a septal (right), anterior, left lateral, and inferior quadrant of the 3D topographic display. For each of the 3D topographic views, a mean algorithm determines the mean activity level in each of these 4 regions, expressed as relative activity levels normalized to the maximum 2% of pixels for the whole heart data set for each of the 3D topographic views. Finally, an algorithm automatically identifies regions of each topographic view that have values that deviate outside 2 SDs or

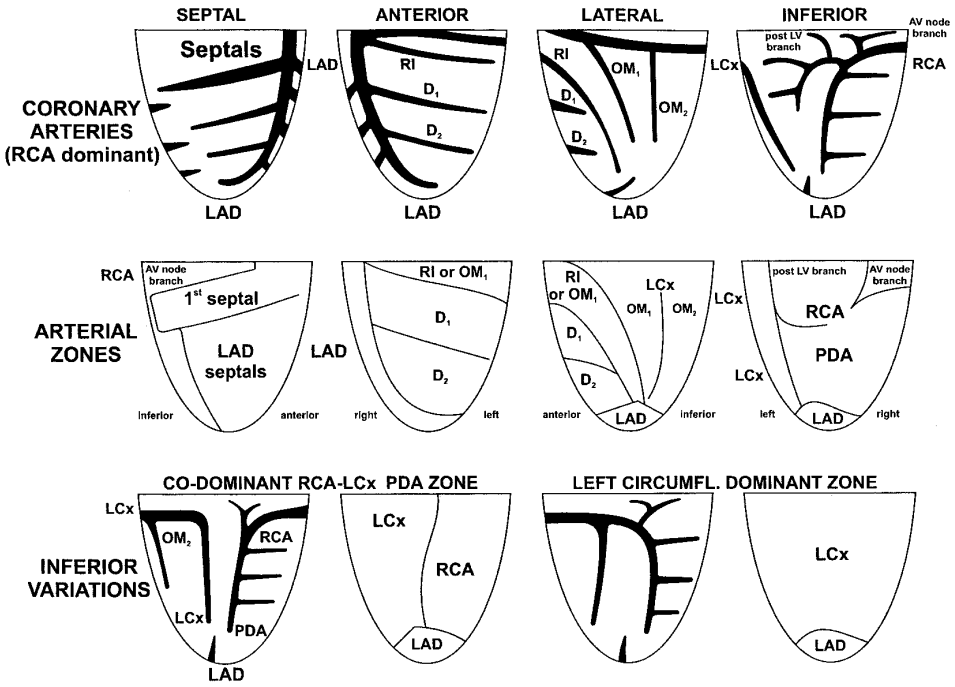

Figure 1. Coronary arteries and myocardial perfusion zones. D_1, First diagonal branch; D_2, second diagonal branch; *AV,* atrioventricular; *RI,* ramus intermedius.

the 95% confidence intervals of normal values based on studies of 17 healthy volunteers aged 23 to 57 years without risk factors of smoking, hypercholesterolemia, hypertension, obesity, diabetes, excessive alcohol or recreational drug use, or family history of coronary artery disease. Of the 4 views only the 3 that illustrate specific perfusion anatomy are shown (in order to minimize article length).

RESULTS: MYOCARDIAL PERFUSION ATLAS AND EXAMPLES

The upper row of Figure 1 illustrates coronary arterial maps superimposed on the 4 quadrant views of the left ventricle and reoriented into the vertical position as is done for tomographic displays of perfusion imaging without the spatial distortion of bull's eye displays. The middle row shows the myocardial perfusion zones corresponding to each coronary artery distribution. The lower row illustrates variations of the posterior-inferior circulation for both arteries and arterial perfusion zones.

Figure 2 illustrates septal, anterior, and lateral views of perfusion defects due to stenoses at different locations in the left anterior descending coronary artery (LAD) and its first septal and first and second diagonal branches in 3 different patients after dipyridamole stress. In the upper panel there is LAD stenosis proximal to the first septal perforator and proximal to all diagonals. The strip of better perfusion at the anterior base is typically supplied by a ramus intermedius or a first obtuse marginal branch (OM_1) of the left circumflex coronary artery (LCx). In the middle panel both the LAD and first septal perforator are open. The first diagonal branch is a large artery with a severe stenosis at its origin. In the lower panel the LAD, the first septal perforator, and the first diagonal branch are open and the second diagonal branch has a severe stenosis at its origin.

Figure 3 shows septal, anterior, and lateral views of perfusion defects due to stenosis in additional locations of the LAD or its branches. The upper panel shows a perfusion defect due to a severe stenosis of the mid LAD distal to the first diagonal branch and proximal to the second diagonal branch. The middle panel shows the perfusion defects due to a moderate stenosis of mid LAD distal to the first diagonal branch and proximal to the second diagonal branch, that has a separate severe stenosis at its origin, thereby making the perfusion defect in the distribution of this branch worse than that of the LAD itself. The lower panel shows a perfusion defect due to a mid LAD occlusion distal to an open diagonal branch. A left internal mammary artery (LIMA) graft to the LAD is patent, but the LAD is diffusely diseased, compromising septal perforators beyond the first septal perforator, which is patent, and thereby creating a moderate perfusion defect in the distribution of the LAD itself and the distal septal branches.

Recurrent angina pectoris after bypass surgery or balloon angioplasty is a problem that may be resolved by

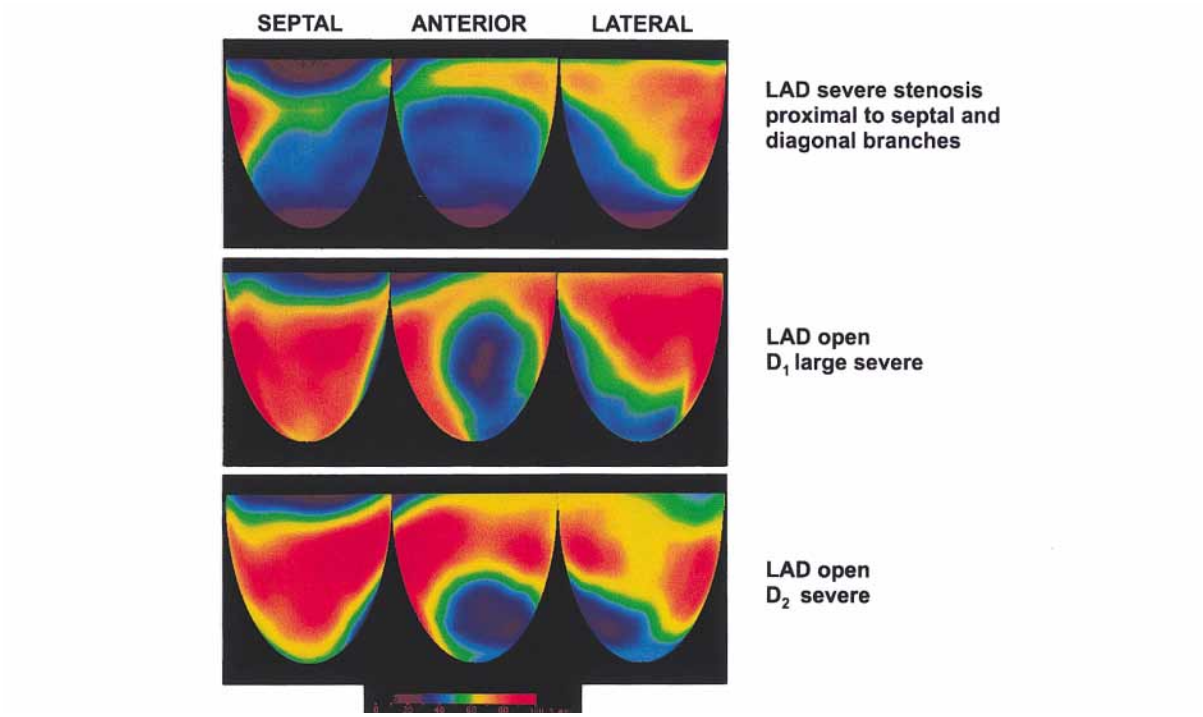

Figure 2. Myocardial perfusion images after dipyridamole in septal, anterior, and lateral views show perfusion defects due to stenoses of the LAD and its branches. D_1, First diagonal branch; D_2, second diagonal branch.

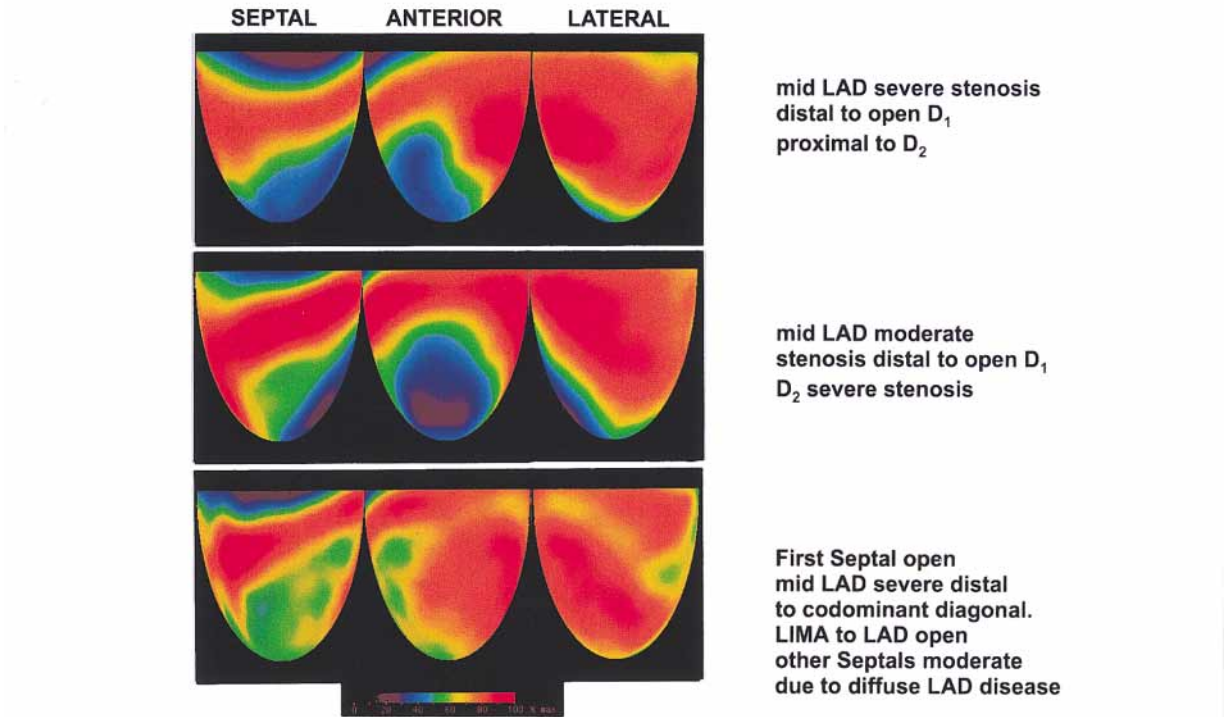

Figure 3. Myocardial perfusion images presented as for Figure 1 for different stenoses of the LAD and its branches. D_1, First diagonal branch; D_2, second diagonal branch.

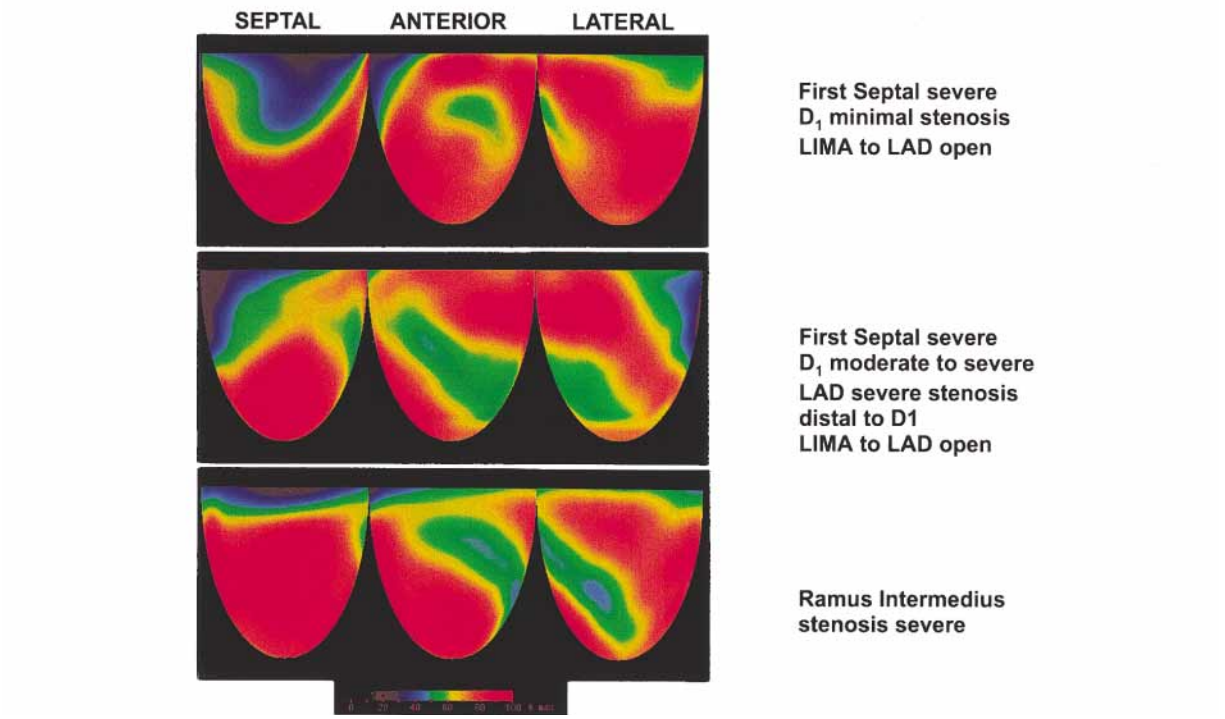

Figure 4. Myocardial perfusion images presented as for Figure 1 for additional stenoses of the LAD and its branches with patent LIMA grafts to LAD. D_1, First diagonal branch.

exact perfusion anatomy as shown by Figure 4 (upper panel). The severe basal septal defect is due to stenosis of the occluded proximal LAD, involving the first septal perforator. The LIMA graft to the LAD distal to the first septal perforator is patent. There is a mild stenosis of the first diagonal branch corresponding to the small, moderate basal anterior defect. The middle panel shows a variation in this pattern of perfusion defects after successful bypass surgery. In this instance the LAD is occluded distal to the first diagonal branch and first septal perforator with a patent LIMA graft to the LAD. Progressive disease then caused stenosis of the proximal LAD, from which the first septal perforator and first diagonal branches arise. We call this pattern the "wasp waist" sign because of the pinching in of perfusion at the basal body of the heart. It is characteristic of recurrent angina with patent grafts after "successful" bypass surgery caused by progressive disease of the LAD and first septal perforator branch proximal to a complete LAD occlusion and patent LIMA. Dipyridamole PET demonstrated this septal perfusion defect as the source of angina, thereby obviating the need for repeat coronary arteriography and further invasive procedures. Even without prior knowledge of bypass procedures, these perfusion patterns are quite specific and are not seen otherwise. The lower panel of Figure 4 shows the perfusion defect due to an isolated ramus intermedius stenosis. The perfusion defect begins at the anteroseptal base and wraps around the anterior and lateral walls to the lateral apex. All other arteries have normal perfusion.

Diagonal branch stenoses typically cause perfusion defects of the anterior wall, whereas LAD defects per se, separate from the diagonal branches, cause septal and anteroseptal defects along the far left edge of the anterior view. Differentiating the diagonal branches from the LAD may be useful for identifying LAD and/or diagonal disease separately or after revascularization procedures that alter flow in the diagonal branches or the LAD separately. Figure 5 illustrates the importance of anatomically distinguishing between LAD and diagonal perfusion defects. The upper panel shows a perfusion defect due to severe LAD stenosis proximal to a large first diagonal branch. Coronary arteriography confirmed this finding and showed that the LAD stenosis also caused a severe stenosis at the origin of a single, large diagonal branch that filled well through collaterals.

Balloon angioplasty and stenting of the LAD were carried out because the diagonal branch was well collateralized. Attempted dilation of the diagonal branch was not successful. The lower panel is a dipyridamole perfusion study in the same patient after successful stenting of the LAD stenosis with complete occlusion of the previously severely stenotic diagonal branch. This follow-up dipyridamole perfusion study indicates a patent LAD,

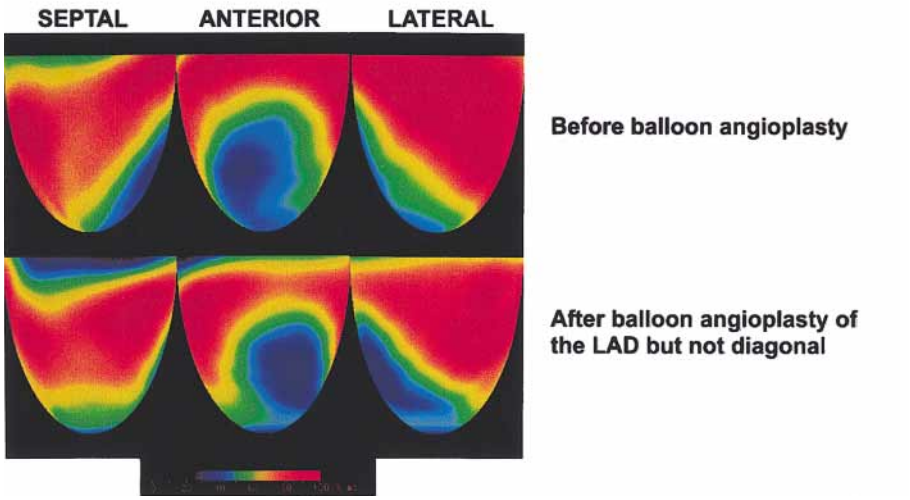

Figure 5. Myocardial perfusion images after dipyridamole before and after balloon angioplasty of LAD with severe stenosis and/or occlusion of codominant diagonal branch.

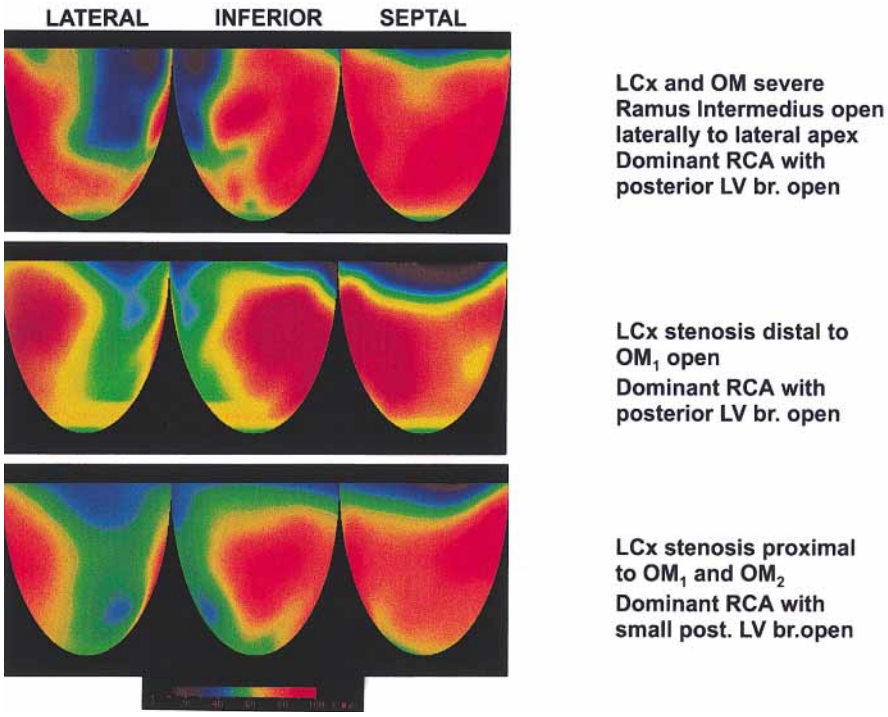

Figure 6. Myocardial perfusion images after dipyridamole in lateral, inferior, and septal views show perfusion defects due to stenoses of LCx, OM_1, and OM_2. *Post. LV br.,* Posterior left ventricular extension branch from the RCA.

although there is a mild apical defect characteristic of diffuse disease. The severity of the perfusion defect in the first diagonal distribution extends more laterally, which is consistent with total occlusion and myocardial steal as observed at the LAD stenting after dipyridamole. Because there were extensive collaterals to the myocardial bed of the first diagonal branch, as demonstrated by both arteriography and PET, no angina, myocardial infarction, or electrocardiographic changes developed and no further procedures were done. With recognition of this diagonal–LAD perfusion pattern, a follow-up arteriogram may be unnecessary in the absence of other clinical indications.

These PET examples show that the LAD is located along the left side of the anterior view and along the right (or anterior) side of the septal or right view. The distal third of the anterior view is the distribution of the second diago-

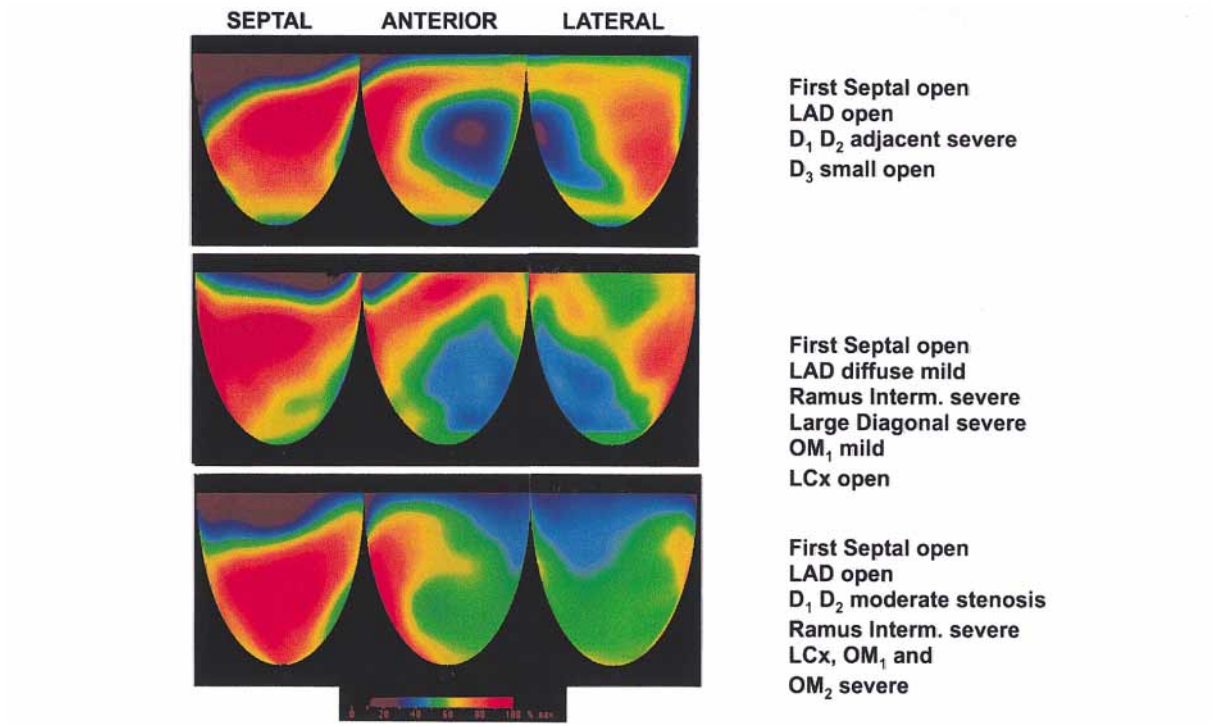

Figure 7. Myocardial perfusion images presented as in Figure 6 for stenoses of various lateral and inferior coronary arteries. *Interm.,* Intermediate; *D_1,* first diagonal branch; *D_2,* second diagonal branch; *D_3,* third diagonal branch.

nal branch. The mid to proximal part of the anterior wall is the distribution of the first diagonal branch, and the base of the anterior wall is the distribution of the ramus intermedius or the OM_1 of the LCx (if there is no ramus intermedius).

Figure 6 illustrates perfusion defects in lateral, inferior, and septal views due to stenoses of the LCx and its obtuse marginal branches. The upper panel shows a perfusion defect due to severe stenosis of the LCx proximal to the only obtuse marginal branch. There is a large, open ramus intermedius to the distal lateral wall. The RCA is dominant with a posterior left ventricular (LV) branch, both of which are patent. The middle panel of Figure 6 illustrates a perfusion defect due to stenosis of the LCx distal to the OM_1. A dominant right coronary artery (RCA) with a posterior LV branch is also patent. The lower panel shows a stenosis of the LCx proximal to the OM_1 and second obtuse marginal branch (OM_2), also with a patent dominant RCA and posterior LV branch. The OM_1 usually distributes well anterior on the lateral view and often to the basal anterior wall.

Figure 7 illustrates several complex multiregion defects due to various combinations of stenoses in the LAD and LCx distribution or their branches. The upper panel shows myocardial perfusion images 6 months after balloon stenting of a stenosis in the LAD near the origins of 2 adjacent diagonal branches. There is a severe defect due to origin stenoses of the 2 adjacent first and second diagonal branches, with a patent LAD and small third diagonal branch. The stenotic diagonal branches extend well into the anterior lateral wall. There is myocardial steal in the distribution of these diagonal branches, indicating good collateralization. Because of good perfusion after dipyridamole in the distribution of the LAD, this artery is widely patent after successful stenting, but the patency of the 2 diagonal branches is compromised.

For the middle panel of Figure 7, the arteriogram shows that the first septal perforator is open; the LAD has mild diffuse disease; a large ramus intermedius and the single, large diagonal branch have severe stenoses; the LCx is open; and the OM_1 is moderately diseased, causing the moderate defect (green area) in the basal lateral region superior to the large severe defect. The anterior and lateral defect is too large for a single branch but does not involve the distribution of the LCx. Therefore it must involve large diagonal branches or large diagonal and ramus intermedius arteries because the defect extends to the lateral apex typical of this latter artery.

The lower panel of Figure 7 shows an extensive perfusion defect, which indicates a patent, diffusely diseased LAD with stenoses of both diagonal branches and the LCx proximal to the obtuse marginal branches. The more

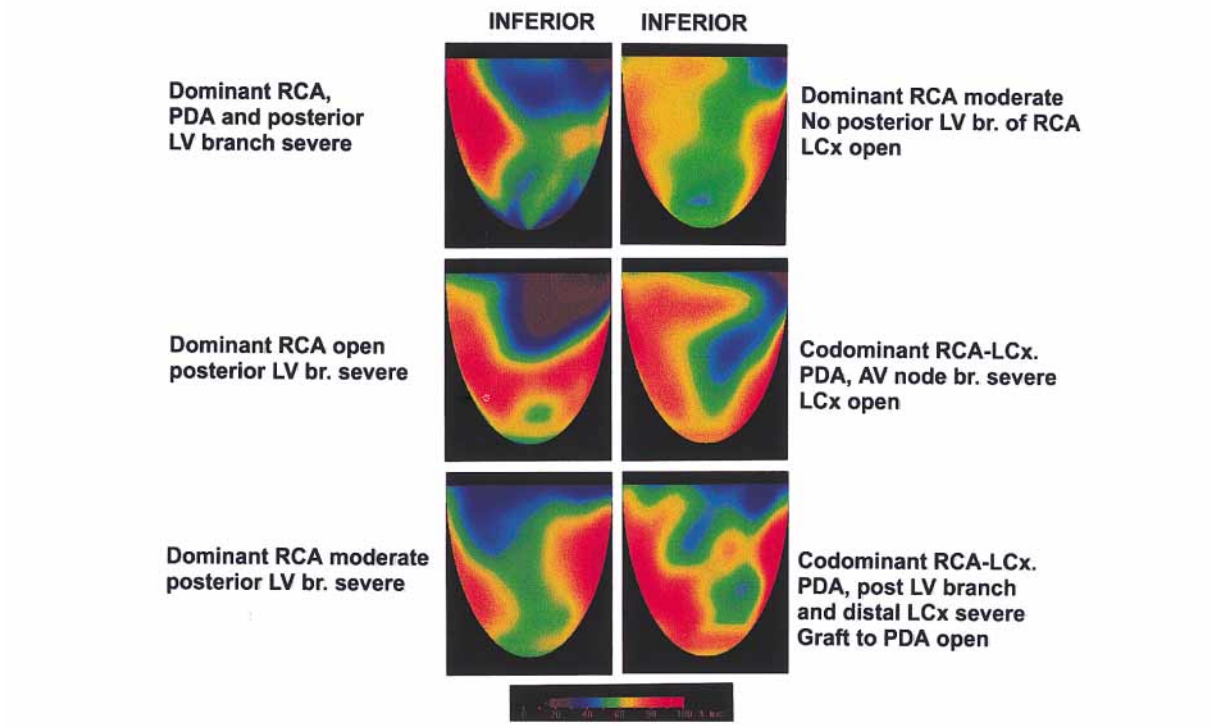

Figure 8. Myocardial perfusion images after dipyridamole in inferior view for stenoses of LCx and RCA in various combinations and for dominance or codominance. *AV,* Atrioventricular; *br.,* branch.

severe blue basal lateral defect indicates a more severe additional stenosis of the OM_1. The RCA with a posterior LV extension branch shows a moderate defect due to diffuse disease, confirmed by coronary arteriography.

Figure 8 illustrates the inferior view of perfusion defects due to stenoses of inferior coronary arteries. The variations include dominant RCA and codominant RCA-LCx supplying the posterior descending coronary artery (PDA), shown both with and without a posterior LV extension branch from the RCA.

Figure 9 shows additional inferior perfusion defects at the extremes of myocardial perfusion anatomy ranging from a large, severe defect caused by severe stenosis of a dominant LCx to the smallest defect caused by disease of an isolated atrioventricular nodal branch at the inferior crux of the left ventricle.

Figure 10 shows lateral, inferior, and septal views of complex perfusion defects due to stenoses of both LCx and RCA. The upper panel shows a perfusion defect due to separate stenoses of the mid ramus intermedius, a mid OM_1, and a mid PDA arising from a patent, dominant RCA with its open posterior LV extension branch. The LCx is also patent. The middle panel shows the perfusion defects due to severe stenoses of the OM_2, the posterior LV extension branch from the RCA, and moderate stenosis of the dominant RCA-PDA. The lower panel shows perfusion defects due to severe stenosis of a dominant RCA-PDA distal to an open posterior LV extension branch. The distal LCx has a severe stenosis beyond the lateral obtuse marginal branches. This pattern of an inferior "double defect" separated by a better-perfused mid inferior zone always indicates stenoses of both LCx and RCA supplying the inferior wall. Recognition of these inferior perfusion patterns (ie, double defects) and distribution more laterally, as opposed to more septally, commonly indicate which artery is dominant to the inferior wall.

Figure 11 shows results for a patient who had recurrent angina pectoris after balloon angioplasty of a severe LCx stenosis at another institution. The PET scan after LCx angioplasty showed a perfusion defect that suggested stenosis of the RCA, but review of the previous outside angiogram results showed no stenosis of this vessel. Because the PET perfusion defect indicated stenosis of a dominant RCA, a follow-up arteriogram was obtained, confirming the LCx to be widely patent with no other stenoses apparent on standard views. However, as a result of the PET scan, special arteriographic views were obtained that revealed a severe right ostial stenosis that was overlooked on routine views of the first arteriogram at initial balloon angioplasty of the LCx. Rotablation and stenting of this right ostial stenosis were successfully car-

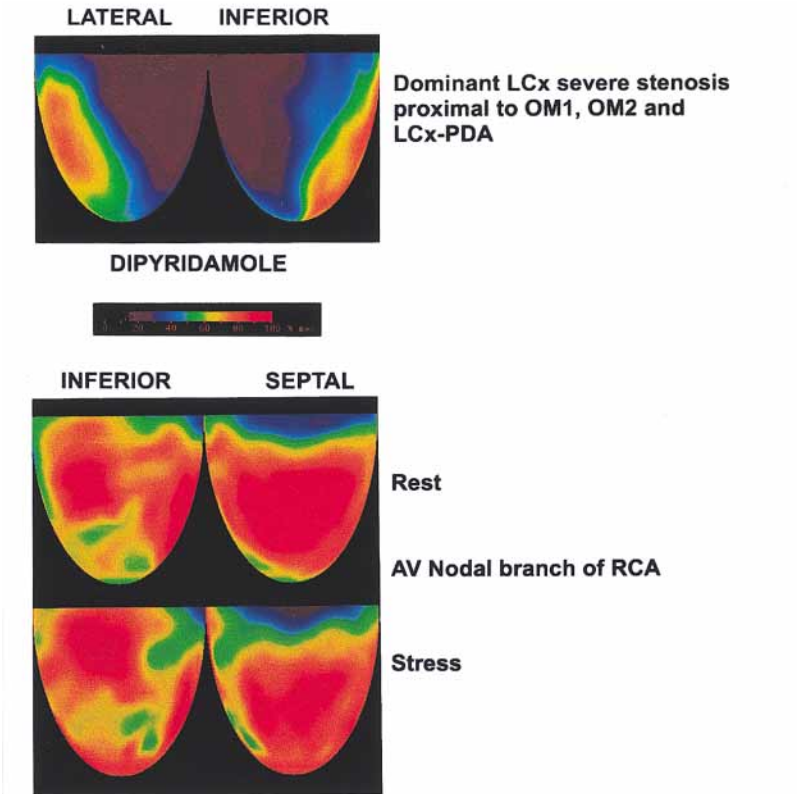

Figure 9. Myocardial perfusion images in lateral and inferior views for stenotic dominant LCx *(upper panel)* and for isolated disease of atrioventricular *(AV)* nodal artery from RCA *(lower panel).*

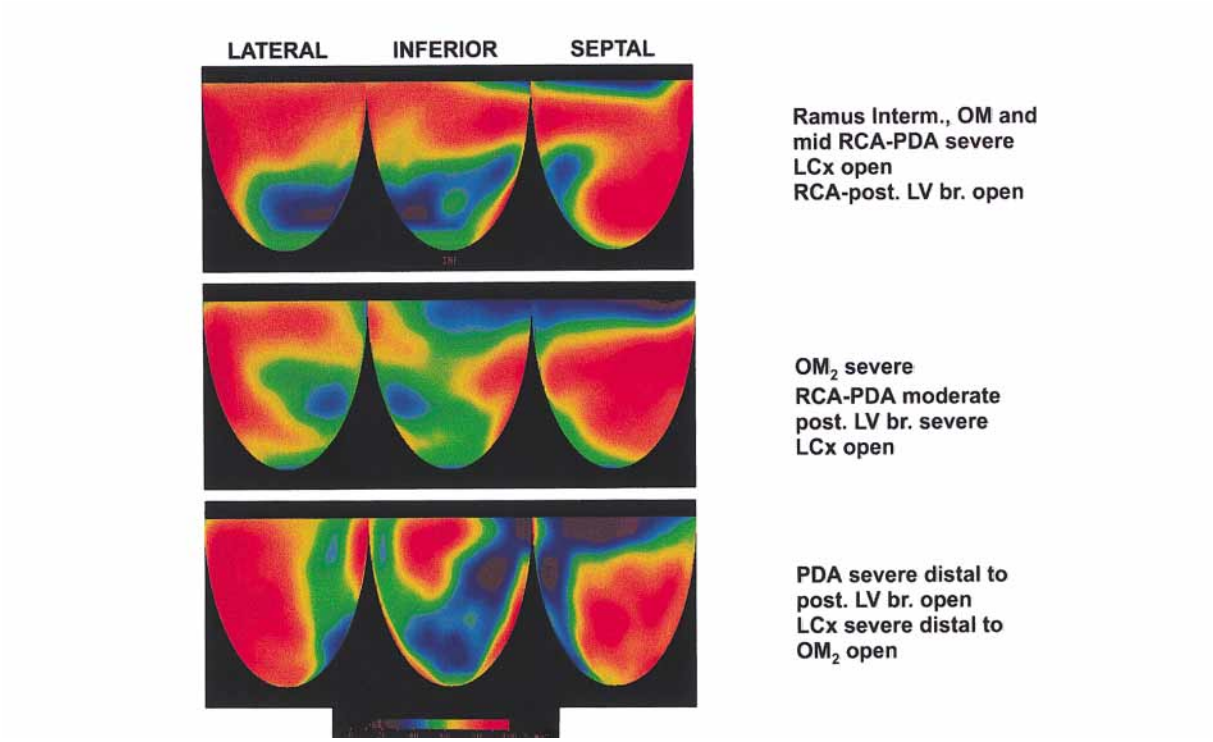

Figure 10. Myocardial perfusion images presented as for Figure 6 for complex perfusion defects due to multiple stenoses of lateral and inferior coronary arteries. *Post. LV br.,* Posterior left ventricular extension branch from the RCA.

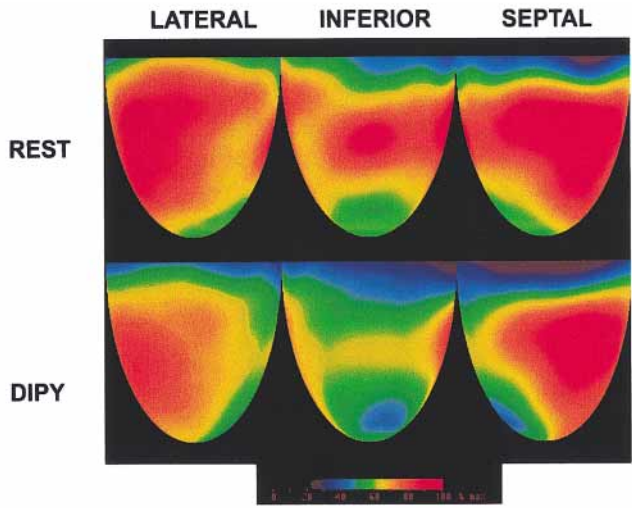

Figure 11. Myocardial perfusion images at rest and after dipyridamole *(DIPY)* in a patient with recurrent angina after successful balloon angioplasty of stenosis of LCx.

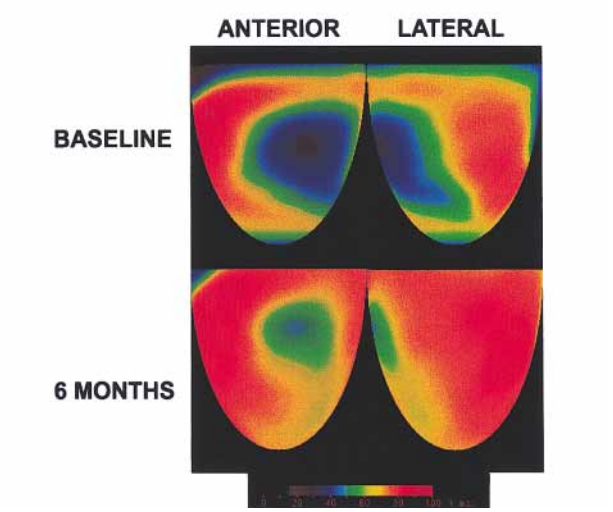

Figure 12. Myocardial perfusion images after dipyridamole before and after 6 months of medical management.

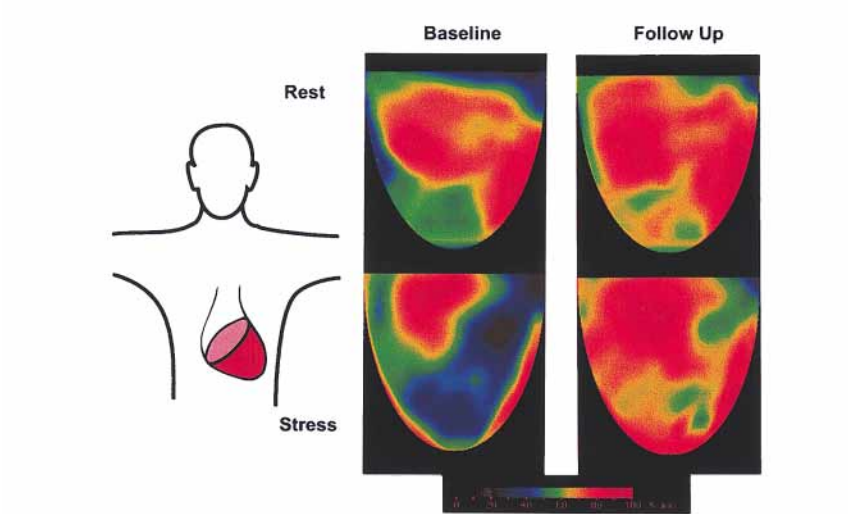

Figure 13. Myocardial perfusion images after dipyridamole before and after 18 months of intense risk factor management.

ried out with disappearance of angina and the PET perfusion defect. As in these examples, precise perfusion anatomy may play a major role in optimizing outcomes and minimizing invasive procedures in the treatment of patients.

Perfusion imaging for following changes in severity may be useful clinically, as illustrated in Figure 12. The severe perfusion defect found 6 months after stenting the LAD indicates procedure-related stenoses at the origins of the 2 adjacent diagonal branches near the stent site (shown in Figure 7). As demonstrated by good perfusion in its distribution, the LAD is widely patent after successful stenting, but with compromised patency of the 2 diagonal branches. The patient had no angina, and ejection fraction during maximal exercise stress as determined by gated blood pool imaging increased from 74% to 82%; this increase in ejection fraction with exercise indicated absence of exercise-induced ischemia due to good collateral perfusion, manifest as myocardial steal on perfusion images after dipyridamole. Intense lipid management[2,14] was therefore continued without repeat revascularization. Six months later follow-up PET revealed substantial improvement, shown in the lower panel of Figure 12.

During the past 10 years, large randomized trials have demonstrated that lipid-lowering improves perfusion and profoundly reduces the risk of coronary events such as myocardial infarction, death, hospitalization, bal-

loon angioplasty, and bypass surgery in patients with established coronary artery disease.[1,2,10-12] Figure 13 illustrates the changes in myocardial perfusion after intense risk factor management, showing marked improvement in perfusion after dipyridamole stress.

References

1. Gould KL. New concepts and paradigms in cardiovascular medicine: the non-invasive management of coronary artery disease. Am J Med 1998;104:2S-17S.
2. Gould KL. Coronary artery stenosis and reversing atherosclerosis. 2nd ed. London: Arnold Publishers; 1999.
3. Mintz GS, Painter JA, Pichard AD, Kent KM, Satler LF, Popma JJ, et al. Atherosclerosis in angiographically "normal" coronary artery reference segments: an intravascular ultrasound study with clinical correlations. J Am Coll Cardiol 1995;25:1479-85.
4. Hausmann D, Johnson JA, Sudhir K, Mullen WL, Friedrich G, Fitzgerald PJ, et al. Angiographically silent atherosclerosis detected in intravascular ultrasound in patients with familial hypercholesterolemia and familial combined hyperlipidemia: correlation with high density lipoproteins. J Am Coll Cardiol 1996;27:1562-70.
5. St Goar FG, Pinto JF, Alderman E, Fitzgerald PJ, Stinson EB, Billingham ME, et al. Detection of coronary atherosclerosis in young adult hearts using intravascular ultrasound. Circulation 1992;86:756-63.
6. RITA-2 Trial Participants. Coronary angioplasty versus medical therapy for angina: the second Randomised Intervention Treatment of Angina (RITA-2) trial. Lancet 1997;350:461-8.
7. Boden WE, O'Rourke RA, Crawford MH, Blaustein AS, Deedwania PC, Zoble RG, et al, for the Veterans Non-Q Wave Infarction Strategies in Hospital (VANQWISH) Trial Investigators. Outcomes in patients with acute non-Q-wave myocardial infarction randomly assigned to an invasive as compared with a conservative management strategy. N Engl J Med 1998;338:1785-92.
8. Pitt B, Waters D, Brown WV, van Boven AJ, Schwartz L, Title LM, et al. Aggressive lipid-lowering therapy compared with angioplasty in stable coronary artery disease. Atorvastatin versus Revascularization Treatment Investigators. N Engl J Med 1999;341:70-6.
9. Brown BG, Brockenbrough A, Zhao X-Q. Very intensive lipid therapy with lovastatin, niacin, and colestipol for prevention of death and myocardial infarction: a 10-year Familial Atherosclerosis Treatment Study (FATS) follow-up [abstract]. Circulation 1998;98:I-635.
10. Demer LL, Gould KL, Goldstein RA, Kirkeeide RL. Diagnosis of coronary artery disease by positron emission tomography: comparison to quantitative coronary arteriography in 193 patients. Circulation 1989;79:825-35.
11. Gould KL, Martucci JP, Goldberg DI, Hess MJ, Edens RP, Latifi R, et al. Short-term cholesterol lowering decreases in size and severity of perfusion abnormalities by positron emission tomography after dipyridamole in patients with coronary artery disease. Circulation 1994;89:1530-8.
12. Gould K, Ornish D, Scherwitz L, Brown S, Edens RP, Hess MJ, et al. Changes in myocardial perfusion abnormalities by positron emission tomography after long-term, intense risk factor modification. JAMA 1995;274:894-901.
13. Xu EZ, Mullani NA, Gould KL, Anderson WL. A segmented attenuation correction for PET. J Nucl Med 1991;32:161-5.
14. Gould KL. Heal your heart: How you can prevent or reverse heart disease. New Brunswick (NJ): Rutgers University Press; 1998.